

Block of Brain Sodium Channels by Peptide Mimetics of the Isoleucine, Phenylalanine, and Methionine (IFM) Motif from the Inactivation Gate

GALEN EAHOLTZ,* ANITA COLVIN,† DANIELE LEONARD,§ CHARLES TAYLOR,||
and WILLIAM A. CATTERALL*‡

From the *Graduate Program in Neurobiology and †Department of Pharmacology, University of Washington, Seattle, Washington 98195-7280; and §Department of Chemistry and ||Department of Neuroscience Therapeutics, Parke-Davis Research Division, Warner-Lambert Co., Ann Arbor, Michigan 48105

ABSTRACT Inactivation of sodium channels is thought to be mediated by an inactivation gate formed by the intracellular loop connecting domains III and IV. A hydrophobic motif containing the amino acid sequence isoleucine, phenylalanine, and methionine (IFM) is required for the inactivation process. Peptides containing the IFM motif, when applied to the cytoplasmic side of these channels, produce two types of block: fast block, which resembles the inactivation process, and slow, use-dependent block stimulated by strong depolarizing pulses. Fast block by the peptide ac-KIFMK-NH₂, measured on sodium channels whose inactivation was slowed by the α -scorpion toxin from *Leiurus quinquestriatus* (LqTx), was reversed with a time constant of 0.9 ms upon repolarization. In contrast, control and LqTx-modified sodium channels were slower to recover from use-dependent block. For fast block, linear peptides of three to six amino acid residues containing the IFM motif and two positive charges were more effective than peptides with one positive charge, whereas uncharged IFM peptides were ineffective. Substitution of the IFM residues in the peptide ac-KIFMK-NH₂ with smaller, less hydrophobic residues prevented fast block. The positively charged tripeptide IFM-NH₂ did not cause appreciable fast block, but the divalent cation IFM-NH(CH₂)₂NH₂ was as effective as the pentapeptide ac-KIFMK-NH₂. The constrained peptide cyclic KIFMK containing two positive charges did not cause fast block. These results indicate that the position of the positive charges is unimportant, but flexibility or conformation of the IFM-containing peptide is important to allow fast block. Slow, use-dependent block was observed with IFM-containing peptides of three to six residues having one or two positive charges, but not with dipeptides or phenylalanine-amide. In contrast to its lack of fast block, cyclic KIFMK was an effective use-dependent blocker. Substitutions of amino acid residues in the tripeptide IFM-NH₂ showed that large hydrophobic residues are preferred in all three positions for slow, use-dependent block. However, substitution of the large hydrophobic residue diphenylalanine or the constrained residues phenylglycine or tetrahydroisoquinoline for phe decreased potency, suggesting that this phe residue must be able to enter a restricted hydrophobic pocket during the binding of IFM peptides. Together, the results on fast block and slow, use-dependent block indicate that IFM peptides form two distinct complexes of different stability and structural specificity with receptor site(s) on the sodium channel. It is proposed that fast block represents binding of these peptides to the inactivation gate receptor, while slow, use-dependent block represents deeper binding of the IFM peptides in the pore.

KEY WORDS: sodium channel • inactivation • gating • peptides • ion channels

INTRODUCTION

Voltage-gated sodium channels open transiently in response to depolarization of the membrane. The transient nature of the sodium current is a function of two distinct gating processes that take place on the millisecond time scale: activation followed by inactivation. So-

dium channels from mammalian brain are a heterotrimeric complex of α (260 kD), β 1 (36 kD), and β 2 (33 kD) subunits (Catterall, 1992). The cloned type IIA α subunit of brain sodium channels consists of four homologous domains, each containing six hydrophobic transmembrane segments and a pore-forming loop (Noda et al., 1986; Auld et al., 1988, 1990; for reviews see Catterall, 1992; Patlak, 1991). The cytoplasmic loop between homologous domains III and IV (L_{III-IV}) is required for the inactivation process, as shown by experiments with site-specific antibodies (Vassilev et al., 1988, 1989) and mutants with cuts or deletions in this intracellular loop (Stühmer et al., 1989; Patton et al., 1992). Mutation of the hydrophobic amino acids isoleucine,

Dr. Eaholtz's present address is Department of Physiology and Biophysics/HHMI, University of Washington, Seattle, WA 98195-7370.

Address correspondence to William A. Catterall, Ph.D., Department of Pharmacology, University of Washington, Box 357280, Seattle, WA 98195-7280. Fax: 206-685-3822; E-mail: wcatt@u.washington.edu

phenylalanine, and methionine (IFM)¹ at positions 1488–1490 to gln disrupts inactivation without affecting activation, and inactivation is nearly completely lost when only Phe1489 is mutated to gln (F1489Q; West et al., 1992; Kellenberger et al., 1996). The IFM-containing peptide acetyl-KIFMK-NH₂ (ac-KIFMK-NH₂) rapidly blocks open F1489Q mutant channels having disrupted inactivation and mimics several features of the intrinsic inactivation process (Eaholtz et al., 1994). IFM-containing peptides also block wild-type sodium channels with functional inactivation and produce large tail currents, suggesting that bound ac-KIFMK-NH₂ prevents closure of the inactivation gate (Eaholtz et al., 1994). The structural specificity of peptide block follows that for function of the inactivation gate itself (Eaholtz et al., 1994).

In inside-out patches containing mutant sodium channels whose intrinsic inactivation was disrupted by the mutation F1489Q, the peptide ac-KIFMK-NH₂ produced a fast block through a bimolecular reaction with the channel with an apparent affinity of 33 μ M (Eaholtz et al., 1994, 1998). A second, slow block was observed during repetitive depolarizations and was slow to reverse (Eaholtz et al., 1994). This slow, use-dependent block resembles block of native sodium channels by local anesthetics (for review see Buttersworth and Strichartz, 1990; Hille, 1992). In these experiments, we have investigated the structural requirements for fast peptide block and slow, use-dependent peptide block of sodium channels. Our results demonstrate the importance of peptide charge, hydrophobicity, and conformation in determining the specificity of block of sodium channels and suggest that fast block and slow use-dependent block represent formation of distinct complexes with different kinetics, voltage dependence, and structural specificity.

MATERIALS AND METHODS

Synthesis and Purification of Peptides

Peptides were synthesized by the solid phase method and purified to a single peak by reverse-phase HPLC on a C18 column (Waters Associates, Millipore Corp.). Purity was determined by mass spectrometry (Department of Biochemistry, University of Washington) and amino acid analysis (AAA Laboratory). In some cases, elemental analysis was done by Parke-Davis, Warner Lambert Co. Peptides were lyophilized and stored at -20°C until needed for physiological experiments.

Cell Culture

All experiments were performed on the alpha subunit of type IIA sodium channels stably expressed in Chinese hamster ovary cells to yield the cell-line CNaIIA (West et al., 1992). Typically, cells were dissociated using 0.25% trypsin (Worthington Biochemical Corp.) in a standard phosphate-buffered saline solution. Cells were seeded at low density onto 35-mm tissue culture plates (Corning Glass

Works) using RPMI media (ICN Biomedicals Inc.) supplemented with 10% fetal calf serum (Hyclone), 20 $\mu\text{g}/\text{ml}$ streptomycin, and 10 $\mu\text{g}/\text{ml}$ penicillin (Sigma Chemical Co.). Electrophysiological recordings of cells were made starting 24 h after subculture.

Recordings

The whole-cell configuration of the patch-clamp recording technique was used (Hamill et al., 1981). All recordings were performed at room temperature ($22\text{--}25^{\circ}\text{C}$). Electrodes were pulled from glass hematocrit tubes (75 μl ; VWR Scientific Corp.) and polished to resistances of 0.5–1.0 M Ω when filled with the pipette solution. Whole-cell macroscopic currents were measured using an EPC-7 patch clamp amplifier (List Medical/Medical Systems). The settling time of the clamp before compensation was <100 μs . The series resistance in the whole-cell configuration was <2 M Ω as measured by the EPC-7 amplifier circuitry, and at least 50% of this was compensated by the patch clamp circuitry. The amplifier output was low-pass filtered through an eight-pole Bessel filter at 7 kHz (Frequency Devices, Inc.), digitized at 20 μs per point, and data were stored on computer disks for later analysis. Voltage protocols were controlled by a computer equipped with an Indec analogue to digital converter (Indec Systems) running the Indec BASIC-Fastlab software. The uncompensated capacitance and leakage currents were subtracted using P/–4 voltage protocols (Bezanilla and Armstrong, 1977). Data analysis was done using Sigma Plot (Jandel Scientific Corp.) running on a 386 computer and IGOR software (Wave Metrics) running on an Apple Macintosh Quadra 800. Unless otherwise indicated, all data are reported as mean \pm SEM.

Solutions

The pipette solution consisted of (mM): 130 CsF, 10 NaCl, 10 HEPES (Calbiochem Corp.), 10 EGTA (Sigma Chemical Co.), pH 7.35 with CsOH. The bath solution contained (mM): 150 NaCl, 5 KCl, 1.5 CaCl₂, 1.0 MgCl₂, 10 HEPES, pH 7.4 with KOH. All solutions were filter sterilized. The lyophilized peptides were dissolved in the internal solution at a concentration of 1 mM unless stated otherwise. Solutions were stored at 4°C for up to 2 wk. To remove inactivation, the α -scorpion toxin from *Leiurus quinquestriatus* (LqTx; Catterall, 1976) was added to the bathing solution at a final concentration of 100 nM.

Diffusion Time of Peptides

Peptides were dissolved in the pipette solution and applied to the cytoplasmic surface of the cell membrane by diffusion through the recording pipette after the whole-cell recording configuration was established (Eaholtz et al., 1994). The time constant of diffusion for ac-KIFMK-NH₂ from the pipette into the cytoplasm was calculated using the methods of Pusch and Neher (1988) from the size of the molecule (expressed as molecular weight), the access resistance, and the cell size (determined from capacitance measurements). The peptide ac-KIFMK-NH₂ has a mol wt of ~ 706 D. With a measured access resistance of $R_A = 1.63 \pm 0.09$ ($n = 32$), diffusion of ac-KIFMK-NH₂ would have a time constant of 47.7 s. Thus, steady state conditions should be reached within ~ 4 min. Our experiments were started 8–12 min after the whole-cell configuration had been established to ensure that the peptide had completely dialyzed into the cell.

Measurement of Blocking Rates Induced by Peptides

Blocking and unblocking rates of the peptides to LqTx-modified sodium channels were measured from the decay in the macroscopic currents elicited by voltage steps to 0 mV from a -80-mV

¹Abbreviations used in this paper: IFM, isoleucine, phenylalanine, and methionine; LqTx, *Leiurus quinquestriatus*.

holding potential. Currents were fitted by a single exponential function following the methods described by Murrell-Lagnado and Aldrich (1993) [see also Patton et al. (1993) and Eaholtz et al. (1998)]:

$$I_{0mv} = B + A \exp^{(-t/\tau)}, \quad (1)$$

where τ is the time constant of peptide-induced block, A is the decaying component of the current due to peptide block extrapolated back to time zero at the beginning of the applied voltage step, and B is the magnitude of current not blocked by peptide at steady state. The fractional steady state current (F_{ss}) was calculated as $F_{ss} = B/(A + B)$. The values for F_{ss} and τ were used to calculate the blocking (k_b) and unblocking (k_u) rates by the following equations:

$$k_{b0} = \frac{(1 - F_{ss})}{\tau_{fast}} \quad (2)$$

and

$$k_{u0} = \frac{F_{ss}}{\tau_{fast}}. \quad (3)$$

The blocking rates were all measured at 1-mM peptide concentration unless otherwise indicated. The τ and F_{ss} values, as well as the blocking (k_{b0}) and unblocking (k_{u0}) rates measured from the currents elicited by a 0-mV pulse, were compared for different peptides.

Measurement of Use-dependent Block

Use-dependent block was the cumulative decrease in current in the presence of intracellular IFM peptides that occurred when large depolarizing voltage steps were given at high frequency. Use-dependent block induced by IFM peptides was measured using a voltage protocol described by Cahalan (1978) for studying use-dependent block of sodium channels by local anesthetics. This protocol consisted of a series of 12 voltage pulses: a single 10-ms control pulse to 0 mV (pulse 1), followed by ten 10-ms conditioning pulses to a depolarizing voltage, and then a final test pulse to 0 mV (pulse 12; see Fig. 4 B, inset). The fraction of remaining sodium current was determined from the ratio of the peak currents elicited from test pulse relative to the initial control pulse (I_{12}/I_1).

The voltage dependence of use-dependent block by ac-KIFMK-NH₂ was determined by varying the voltage of the conditional pulses over the range from -50 to 200 mV. The fraction of remaining current was plotted as a function of conditioning pulse voltage, and the data were fitted to the equation (Cahalan, 1978):

$$\frac{I_{test}}{I_{control}} = \frac{1}{1 + \exp^{(V - V_{1/2})/s}}, \quad (4)$$

where V is the voltage of the conditional pulses, $V_{1/2}$ is the voltage of half-maximal block, and s is $RT/z\delta F$, where δ represents the fraction of the electrical potential across the membrane acting on the charged blocker in its binding site, and z is the valence of the blocking peptide (see Cahalan, 1978; Strichartz, 1973; Woodhull, 1973).

RESULTS

Structural Features that Affect Fast Block by IFM Peptides

In our previous experiments, peptides containing the IFM motif in a sequence of seven or more amino acid

residues from L_{III-IV} were found not to produce fast block, suggesting that these peptides are too large to reach their receptor site(s) in a native sodium channel with its intrinsic inactivation gate intact (Eaholtz et al., 1994). Based on those results, small peptides of three to six amino acid residues with different structural properties were investigated in these experiments. We measured the peptide block of sodium channels whose inactivation was inhibited by the α -scorpion toxin from LqTx. Inactivation was inhibited with LqTx rather than by mutation for three reasons: (a) the toxin binds reversibly and can be washed out of the bath to restore inactivation, (b) the toxin inhibits inactivation more effectively than the mutation F1489Q, which shows some residual fast inactivation, and (c) the expression levels of wild-type channels in either mammalian cells or oocyte expression systems are higher than those of the mutant channels F1489Q or IFM1488-1490QQQ. Sodium currents were recorded in the presence of 100 nM LqTx during 10-ms voltage steps from a holding potential of -80 mV to test potentials from -80 to +100 mV, and synthetic peptides were dissolved in the pipette solution at a concentration of 1 mM and internally applied through the recording pipette.

In the absence of any peptide, LqTx-modified currents recorded at 0 mV from the cell illustrated in Fig. 1 decayed with a time constant of 4.6 ms soon after establishment of the whole-cell configuration, compared with 3.9 ms 20 min later (Fig. 1, no peptide). The mean time constant for three cells measured ~15–20 min after seal disruption was 4.1 ± 0.7 ms (Table I), approximately sevenfold slower than unmodified sodium channels. To illustrate the effects of the various peptides tested on the time course of sodium current, the peptide-modified sodium currents recorded from different cells (Fig. 1, solid lines) were superimposed and normalized to the control LqTx-modified sodium current (Fig. 1, dotted current traces). The indicated peptides were all tested at a concentration of 1 mM, and currents from individual cells were recorded at 0 mV ~20 min after establishing the whole-cell voltage clamp configuration. From fits of Eq. 1 to the sodium currents recorded at 0 mV, the time constants and fractional steady state currents were determined for the peptides studied (Table I). Mean blocking and unblocking rates for fast block induced by several of the peptides were calculated using Eqs. 2 and 3 and tabulated in Table I.

Ac-KIFMK-NH₂, with a net charge of +2 contributed by the two lysine residues, produced fast block of the LqTx-modified sodium channels at 0 mV with a mean time constant of 0.35 ± 0.04 ms (Fig. 1, Table I). An average of 21% of the extrapolated peak sodium current ($A + C$, Eq. 1) remained unblocked at steady state (Fig. 1, Table I). Inspection of the superimposed current traces in Fig. 1 gives the impression of a larger fraction

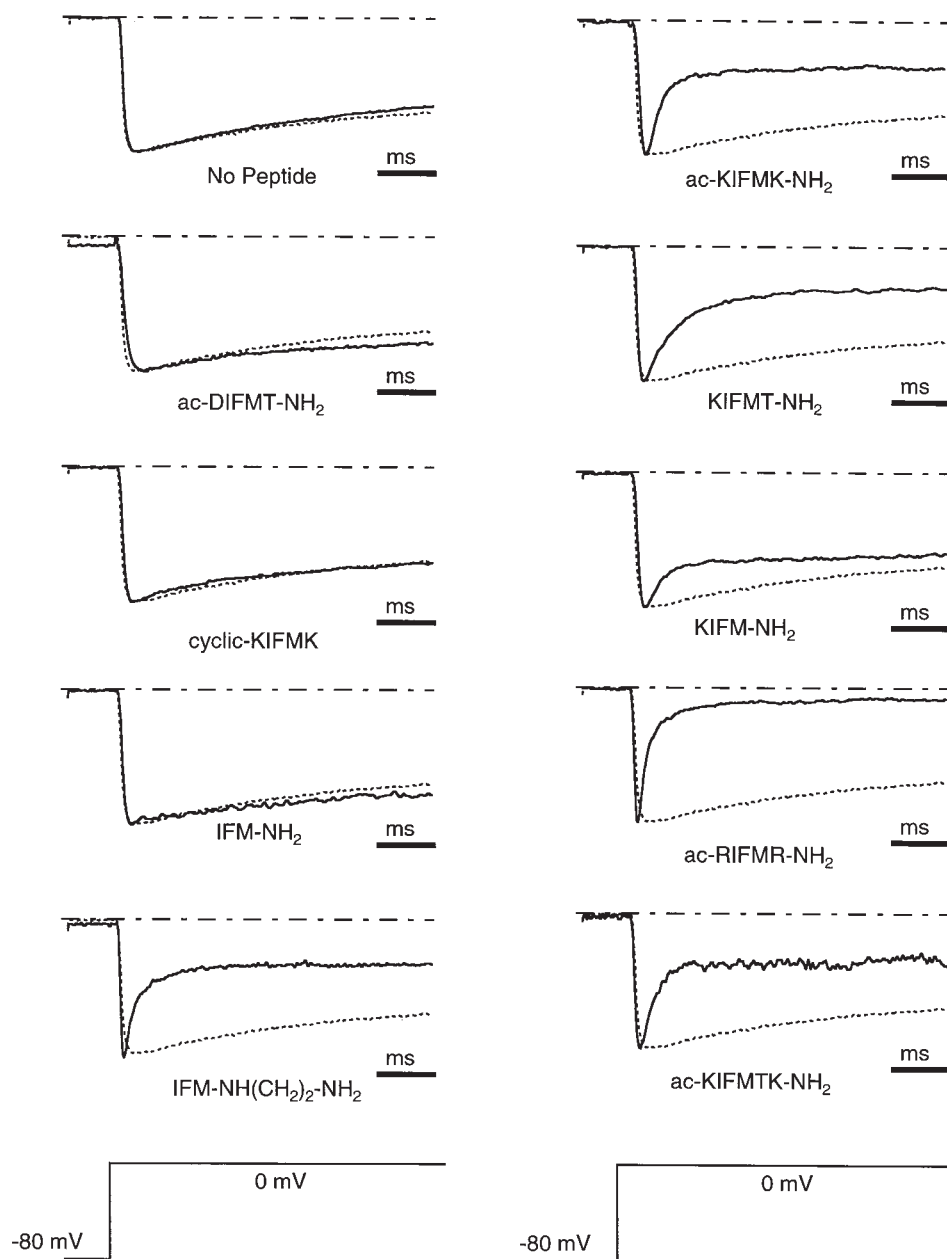


FIGURE 1. Effects of IFM-containing peptides on time course of current through LqTx-modified sodium channels. Sodium currents were elicited by voltage steps to 0 mV from a holding potential of -80 mV. The control (No Peptide) shows superimposed sodium currents from the same cell, in the presence of 100 nM LqTx, 5 (solid line) and 20 (dashed line) min after establishing the whole-cell configuration (top left). Other sodium currents (solid lines) were recorded ~ 20 min after establishing the whole-cell configuration with a recording pipette containing 1 mM of the indicated peptide. The control (No Peptide) trace (dashed line) is superimposed on the peptide traces. Scale bars indicate 1 ms. The current traces were normalized to the peak sodium current. The peak currents for the traces illustrated were: control, -6.1 nA; ac-DIFMT-NH₂, -3.1 nA; cyclic KIFMK, -6.3 nA; IFM-NH₂, -1.8 nA; IFM-NH(CH₂)₂-NH₂, 3.2 nA; ac-KIFMK-NH₂, -2.4 nA; KIFMT-NH₂, -3.1 nA; KIFM-NH₂, -4.1 nA; ac-RIFMR-NH₂, -3.6 nA; and ac-KIFMTK-NH₂, -1.9 nA.

of steady state current than 21% because the traces are normalized to the recorded peak current in the presence of peptide rather than the larger extrapolated peak current. For seven cells, the mean blocking rate of ac-KIFMK-NH₂ at 0 mV was $2,402 \pm 308$ s⁻¹ and its mean unblocking rate was 587 ± 40 s⁻¹ (Table I).

In contrast to ac-KIFMK-NH₂, the peptide ac-DIFMT-NH₂, which has a net charge of -1 and contains an NH₂-terminal asp and a COOH-terminal thr found in the cDNA sequence (Noda et al., 1986; Auld et al., 1988), did not produce significant fast block (Fig. 1). The pentapeptides KIFMT-NH₂ and ac-RIFMR-NH₂, which both have a net charge of $+2$, rapidly blocked LqTx-modified sodium currents (Fig. 1). Compared with ac-KIFMK-NH₂, ac-RIFMR-NH₂ had a faster mean

blocking rate of $3,348 \pm 100$ s⁻¹ and a slower mean unblocking rate (222 ± 33 s⁻¹; $n = 3$) at 0 mV, and therefore produced more steady state block, while the peptide KIFMT-NH₂ had a slower mean blocking rate of $1,169 \pm 108$ s⁻¹ and a faster mean unblocking rate of 386 ± 81 s⁻¹ ($n = 3$) and produced less steady state block at 0 mV. Both ac-RIFMR-NH₂ and ac-KIFMK-NH₂ have positive charges at each end of the peptide, while the net $+2$ charge in KIFMT-NH₂ is localized to the NH₂ terminal. These results indicate that fast block is effective when IFM pentapeptides have two positively charged residues, but the location of the charges within the peptide is less important for the effect.

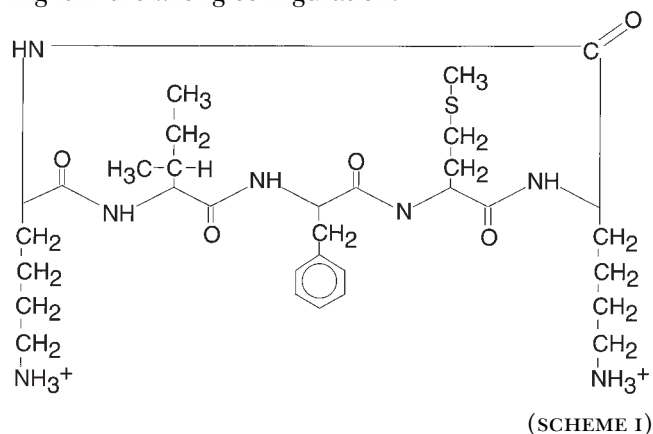
An additional pentapeptide was synthesized that constrained the amino acids KIFMK in a cyclic ring (cyclic-

TABLE I
Fast Peptide Block of LqTx-modified Sodium Channels

Peptide	$\tau_{(0 \text{ mV})}$	FSS _(0 mV)	$k_b(0 \text{ mV})$	$k_u(0 \text{ mV})$	z	n
	ms		s^{-1}	s^{-1}		
LqTx	4.1 ± 0.7					3
ac-RIFMR-NH ₂	0.28 ± 0.01	0.06 ± 0.01	3348 ± 100	222 ± 33	2+	3
ac-KIFMK-NH ₂	0.35 ± 0.04	0.21 ± 0.03	2402 ± 308	587 ± 40	2+	7
ac-KIFMTK-NH ₂	0.28 ± 0.02	0.20 ± 0.01	2881 ± 263	731 ± 8	2+	3
KIFMT-NH ₂	0.67 ± 0.11	0.25 ± 0.01	1168 ± 181	386 ± 81	2+	3
KIFM-NH ₂	0.33 ± 0.03	0.42 ± 0.01	1751 ± 163	1283 ± 149	2+	3
IFM-NH(CH ₂) ₂ -NH ₂	0.32 ± 0.02	0.25 ± 0.01	2367 ± 152	782 ± 105	2+	3

The time course of peptide-induced decay of sodium currents was fit to Eq. 1, and the best fit parameters for the indicated number of experiments were averaged to yield the parameters presented.

KIFMK; Scheme I). This peptide did not exhibit significant fast block of LqTx-modified channels, even though it contained the KIFMK sequence of amino acids and a net charge of +2 (Fig. 1). Thus, constraining the conformation of KIFMK abolished fast block. These results suggest that the conformation of the IFM amino acids is important for the binding interaction. The structural constraints on cyclic KIFMK may have hindered binding by making the peptide too rigid or fixing it in the wrong configuration.



A thr is located on the COOH-terminal side of IFM in the sodium channel amino acid sequence (Noda et al., 1986; Auld et al., 1988, 1990). Substituting a thr for the COOH-terminal lys in the peptide KIFMT-NH₂ slowed the time constant for block twofold relative to ac-KIFMK-NH₂ (Fig. 1, Table I). The peptide ac-KIFMTK-NH₂ was synthesized to determine if a larger peptide with positive charges at each end would be more effective at blocking channels than the smaller KIFMT-NH₂ peptide with two charges at the NH₂ terminal. Ac-KIFMTK-NH₂ produced slightly more fast block of LqTx-modified currents than KIFMT-NH₂ (Fig. 1) with steady state current values of 0.20 ± 0.014 ($n = 3$) and 0.25 ± 0.012 ($n = 3$), respectively. However, the mean time constant of fast block by ac-KIFMTK-NH₂ at 0 mV was 0.28 ± 0.02 ms ($n = 3$), which was more than twofold faster than KIFMT-NH₂ (Table I). Both the mean block-

ing and unblocking rates at 0 mV were faster for ac-KIFMTK-NH₂ relative to KIFMT-NH₂ and were similar to ac-KIFMK-NH₂. These results indicate that ac-KIFMTK-NH₂ is as effective a fast blocker as ac-KIFMK-NH₂.

We also investigated the blocking potency of smaller peptides to determine the minimum IFM-containing structure that would cause fast block. The tetrapeptide KIFM-NH₂, with a net charge of +2, induced fast block with a mean time constant of 0.33 ± 0.03 ms for three cells (Fig. 1, Table I). The fractional steady state current, 42%, was larger for KIFM-NH₂ than that observed for the pentapeptides due to the faster unblocking rate of KIFM-NH₂. It appeared that KIFM-NH₂ was less stably bound than the pentapeptides containing the IFM sequence and two positive charges. The more stable binding of the larger peptides suggested that additional interactions may be involved in stabilizing the peptide in the channel pore.

The blocking effectiveness of IFM tripeptides was also investigated. IFM-NH₂ carries a net charge of +1 at the NH₂ terminal and is readily soluble in the recording solution. It did not rapidly block LqTx-modified channels (Fig. 1). However, the peptide IFM-NH(CH₂)₂-NH₂ (Fig. 1, Table I), with two positive charges, was much more effective than IFM-NH₂. Both the mean blocking rates and the unblocking rates at 0 mV of IFM-NH(CH₂)₂-NH₂ were similar to those determined for ac-KIFMK-NH₂. Altogether, these results show that fast block of open sodium channels requires the IFM sequence in a three- to six-residue peptide having two positive charges and sufficient flexibility to adopt an optimal conformation for access and binding to the receptor site. The IFM residues themselves appear to be sufficient for fast block if they are contained in a peptide with two positive charges.

Reversal of Fast Peptide Block

If fast peptide block resembles the intrinsic inactivation process, it would be expected that the kinetics of reversal of inactivation and reversal of peptide block would be similar. The recovery time constants for ac-KIFMK-

NH₂-induced fast block and for intrinsic inactivation of unmodified sodium channels were measured using a standard two-pulse voltage protocol in which the recovery interval at hyperpolarizing voltages was incrementally increased (see Fig. 2, legend). Fig. 2 shows examples of recovery from inactivation in a cell in which sodium channels were not modified by toxin (Fig. 2 A) and recovery from block by 1 mM ac-KIFMK-NH₂ in a cell where channels were modified by LqTx (Fig. 2 B). After a depolarizing pulse to 0 mV to inactivate sodium channels either by closure of the inactivation gate or by binding of peptide, the fractional recovery of sodium current (I_2/I_1) was plotted as a function of the recovery time interval. Recovery from inactivation at -80 mV had a mean time constant of 4.4 ± 0.6 ms ($n = 9$ cells) for unmodified channels (Fig. 2 A), while recovery from ac-KIFMK-NH₂-induced block of LqTx-modified channels was 4.9-fold faster with a time constant of 0.9 ± 0.3 ms ($n = 5$ cells) (Fig. 2 B). When the recovery voltage between the two pulses was made more negative, the time course of recovery was more rapid for both inactivation and peptide block (Fig. 2). These results indicate that bound ac-KIFMK-NH₂ was approximately fivefold less stable than the intrinsic inactivation particle, but responded to voltage changes similarly.

Use-dependent Block of Sodium Channels by ac-KIFMK-NH₂

In our previous experiments, we found that ac-KIFMK-NH₂ and other IFM peptides cause two kinds of sodium channel block, fast block that mimics the intrinsic inactivation process and slow, use-dependent block that occurred during multiple strong depolarizations and reversed much more slowly than inactivation (Eaholtz et al., 1994). Fig. 3 illustrates fast block and slow use-dependent block induced by 1.0 mM ac-KIFMK-NH₂ intracellularly applied to LqTx-modified sodium channels. Ac-KIFMK-NH₂ induces fast, time-dependent decay in LqTx-modified sodium currents during a single voltage step (Fig. 3, left) and a slower cumulative decrease in the peak current amplitude that is voltage- and frequency-dependent when strong depolarizing pulses are given at a frequency above 1 Hz (Fig. 3, right). Slow, cumulative block is more similar in kinetics and voltage dependence to block of sodium channels by local anesthetics.

Voltage Dependence of Use-dependent Block Induced by IFM Peptides

We used a conditioning pulse protocol (Fig. 4, inset) to measure the voltage dependence of use-dependent peptide block induced in wild-type sodium channels with intact inactivation. The mean fractional current (I_{12}/I_1) was plotted versus the voltage of the conditioning pulses for cells in the absence or presence of peptide (Fig. 4 A). For 16 cells not containing peptide,

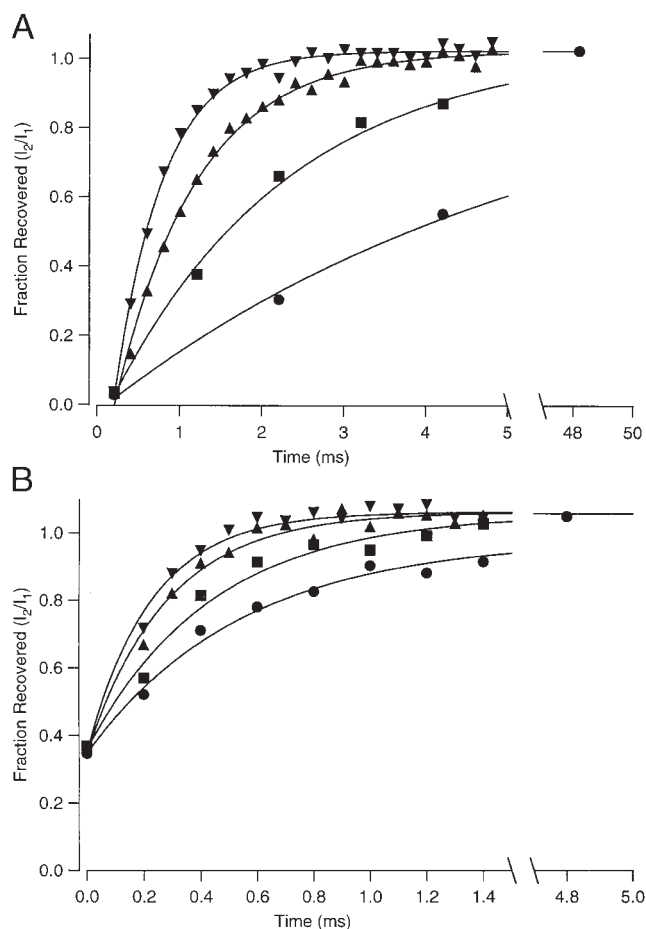


FIGURE 2. Kinetics of recovery from inactivation and from fast block by ac-KIFMK-NH₂. Two 10-ms test pulses to 0 mV separated by repolarization to -80 mV for a variable time interval were used to measure the time course of recovery from (A) inactivation of wild-type channels or (B) ac-KIFMK-NH₂-induced fast block of LqTx-modified channels. Peak current was measured during the two 0-mV test pulses, and the fractional current recovered was determined as the ratio of these two currents, I_2/I_1 . The voltage protocol was repeated 20 \times , and with each repeat the interpulse interval between the two 0-mV pulses was increased incrementally by a time Δt . Recovery at different voltages was tested by setting the voltage during the interpulse interval at -80, -100, -120, and -140 mV. The fractional current was plotted against the time interval separating the two pulses. The fractional current recovered exponentially and the data were fit by a single exponential function to determine the time constants of recovery. (A) An example from a single cell of recovery from fast inactivation of unmodified sodium channels where the interpulse interval was -80 mV (\bullet , $\Delta t = 2$ s), -100 mV (\blacksquare , $\Delta t = 1$ s), -120 mV (\blacktriangle , $\Delta t = 200$ μ s), and -140 mV (\blacktriangledown , $\Delta t = 200$ μ s). Mean values for the recovery from fast inactivation were as follows: -80 mV, $\tau = 4.4 \pm 0.6$ ms ($n = 9$); -100 mV, 1.9 ms ($n = 2$); -120 mV, 0.89 ± 0.06 ms ($n = 9$); -140 mV, 0.85 ± 0.2 ms ($n = 4$). (B) An example from a single cell of recovery from ac-KIFMK-NH₂ block of LqTx-modified sodium channels. The potentials during the interpulse interval were -80 mV (\bullet , $\Delta t = 200$ μ s), -100 mV (\blacksquare , $\Delta t = 200$ μ s), -120 mV (\blacktriangle , $\Delta t = 100$ μ s), and -140 mV (\blacktriangledown , $\Delta t = 100$ μ s). Mean values of the time constants for recovery from block were as follows: -80 mV, $\tau = 0.9 \pm 0.3$ ms ($n = 5$); -100 mV, 0.6 ± 0.1 ms ($n = 6$); -120 mV, 0.4 ± 0.1 ms ($n = 6$); -140 mV, 0.3 ± 0.1 ms ($n = 4$).

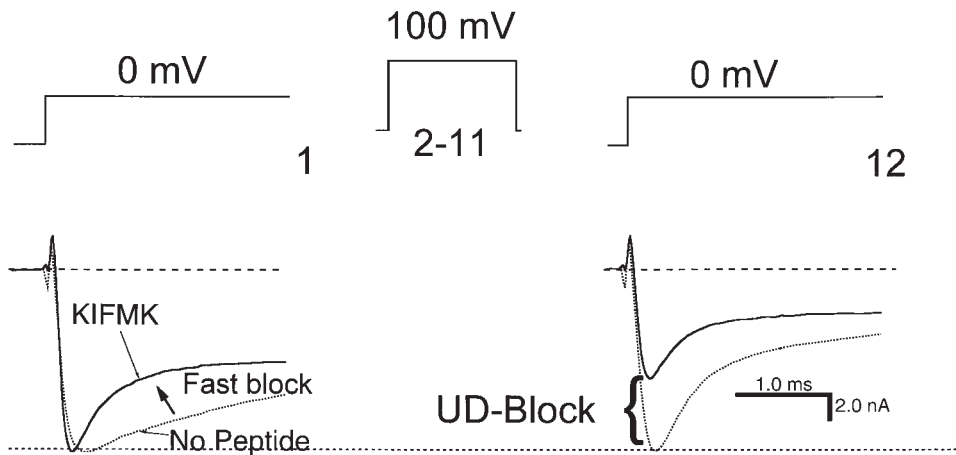


FIGURE 3. Measurement of use-dependent block by ac-KIFMK-NH₂. From a holding potential of -80 mV, a test pulse to 0 mV for 10 ms was applied, followed by 10 conditioning pulses to +100 mV for 10 ms at 10 Hz, and a final test pulse to 0 mV for 10 ms. Sodium currents from LqTx-modified channels were recorded during the two test pulses in the presence or absence of ac-KIFMK-NH₂. (Left) The change in time course of the sodium current in the presence of ac-KIFMK-NH₂ compared with the control current during the first pulse is defined as fast block. (Right) The

decrease in the peak current amplitude between the first and last pulse is defined as use-dependent block (UD-Block). The fast-inactivating component of sodium current in the use-dependent block protocol reflects partial loss of bound α -scorpion toxin during the series of conditioning pulses. This does not significantly affect the measurement of peak sodium current on which our estimates of use-dependent block are based.

there was no change in the amplitude of the current (Fig. 4 A, ○). However, in three cells, 1.5 mM ac-KIFMK-NH₂ produced nearly 100% block with conditioning pulses more positive than 150 mV (Fig. 4 A, ●). The smooth line represents a fit of Eq. 4 to the ac-KIFMK-NH₂ data using the mean fit parameters for half maximal ($V_{1/2}$) block and z of 91.7 ± 3.3 mV and 1.0 ± 0.05 , respectively. Since this peptide carried two positive charges, the mean z value of 1.0 ± 0.05 ($n = 3$) was divided by two to give a value of 0.50, indicating that the charges in this peptide experienced $\sim 50\%$ of the membrane electrical field when interacting with the peptide-binding site during slow, use-dependent block. In contrast, a δ value of 0.3 was observed for fast block by ac-KIFMK-NH₂ (Eaholtz et al., 1998), suggesting that slow use-dependent block involves deeper binding in the pore.

Ac-KIFMK-NH₂ was applied to unmodified and LqTx-modified channels to determine if use-dependent block was affected by the intrinsic inactivation process. The same conditioning pulse protocol was used to elicit currents from peptide-free cells in the absence and presence of 100 nM extracellular LqTx. These results were compared with cells containing 1.0 mM ac-KIFMK-NH₂ in the absence and presence of LqTx (Fig. 4 B). Peptide-free cells in the absence of extracellular LqTx showed no use-dependent block and the fractional current was 0.99 ± 0.01 ($n = 14$). In contrast, the 200-mV conditioning pulses caused a decrease of $\sim 20\%$ in peak current in the presence of extracellular LqTx. Since we observed no similar decrease in current in the absence of LqTx, this reduction in peak current in the presence of LqTx was presumably due to dissoci-

ation of LqTx from the sodium channels at depolarized potentials, resulting in more rapid inactivation and a reduction of sodium current (Catterall, 1976; Mozhaeva et al., 1979). Internal application of ac-KIFMK-NH₂ to cells in the absence or presence of LqTx caused $>95\%$ use-dependent block, with remaining fractional steady state sodium currents of 0.04 ± 0.02 ($n = 3$) and 0.03 ± 0.02 ($n = 6$), respectively (Fig. 4 B). These results indicate that neither the intrinsic inactivation process nor LqTx prevents the peptide from blocking the channel.

Recovery from use-dependent block was examined by modifying the conditioning pulse protocol so that the recovery interval at -80 mV between the last conditioning pulse and the test pulse was increased to 91 s (Fig. 4 B, inset, arrow). The fractional recovery ($I_{1/2}/I_1$) from ac-KIFMK-NH₂-induced use-dependent block was measured for unmodified and LqTx-modified sodium channels (Fig. 4 C). The average fraction of channels to recover from use-dependent block of LqTx-modified channels was larger than for unmodified sodium channels, 0.56 ± 0.04 ($n = 3$) compared with 0.26 ± 0.05 ($n = 8$), respectively. These results suggest that the intrinsic inactivation process slowed the recovery from use-dependent block, perhaps "trapping" the peptide within the channel pore. Half-maximal recovery from use-dependent block at -80 mV required more than 90 s, whereas recovery from fast block was half complete in 0.9 ms at -80 mV (Fig. 2 B). These results show that two distinct complexes are formed with ac-KIFMK-NH₂: a rapidly reversible complex that forms during single depolarizing pulses and resembles the inactivated state of unmodified sodium channels, and a

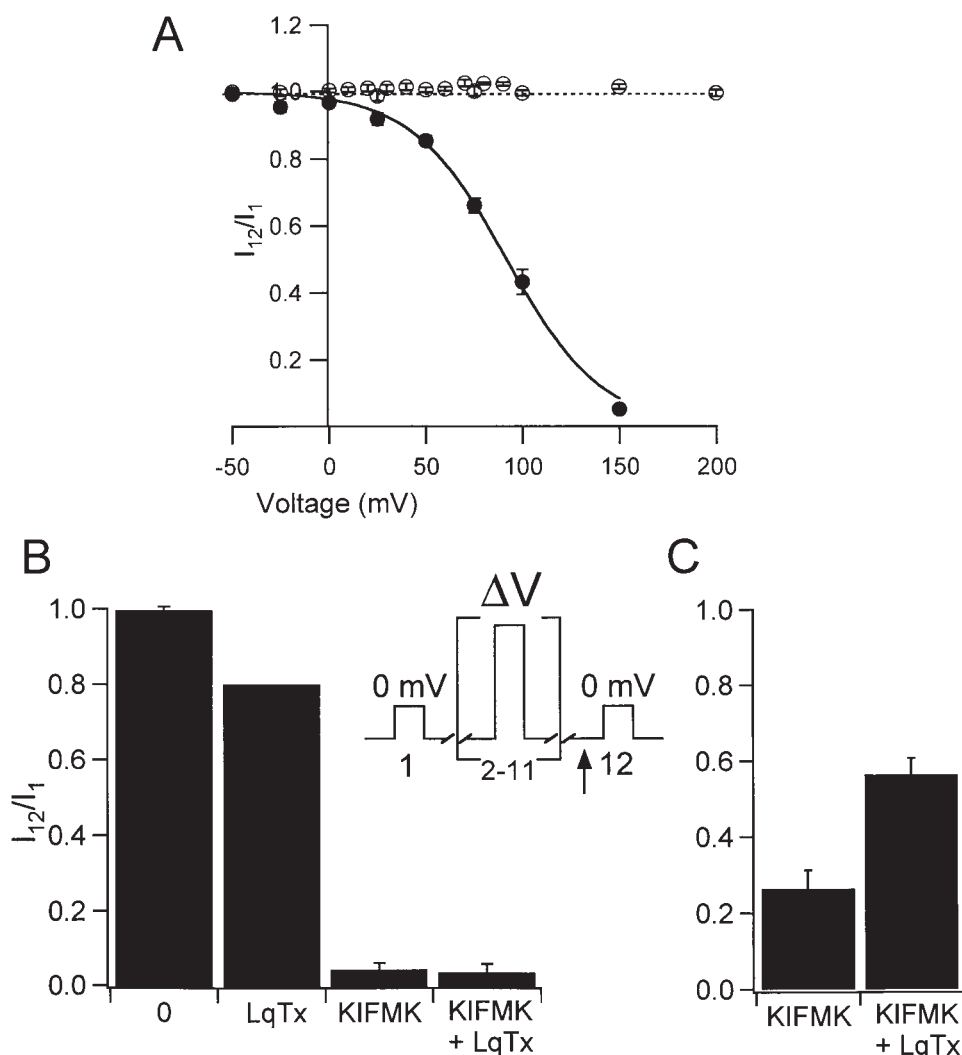


FIGURE 4. Voltage dependence and kinetics of recovery from use-dependent block. (A) Mean fractional current (I_{12}/I_1) was plotted as a function of conditioning pulse voltage (pulses 2–11) for three cells that contained 1.5 mM ac-KIFMK-NH₂ (\bullet), or no peptide (\circ , $n = 16$). The conditioning pulses (V) varied in voltage from -50 to 200 mV from a holding potential of -80 mV. A voltage profile of the conditioning pulse protocol is shown in the inset. Inspection of the sodium currents recorded during the train of conditioning pulses showed that steady state block was reached at each conditioning potential, although the small size of the currents at 50 mV made assessment of steady state less certain at that potential. The smooth line represents fit of the data to Eq. 4 using values for the voltage for half-maximal block and $\alpha\delta$ from the means of individual fits from three cells. The mean voltage at which half the channels were blocked was 91.7 ± 3.3 mV, with a $\alpha\delta$ value of 1.0 ± 0.05 , $n = 3$. (B) The fractional current (I_{12}/I_1) remaining after 10 conditioning pulses was measured for unmodified channels with no peptide, sodium channels modified by LqTx with no peptide, wild-type channels with 1 mM ac-KIFMK-NH₂, and LqTx-modified channels with 1 mM ac-KIFMK-NH₂ in

response to conditional pulses to 200 mV. The mean fractional current for the control with no additions was 0.99 ± 0.01 ($n = 14$); for LqTx-modified, 0.79 ($n = 2$); for 1 mM ac-KIFMK-NH₂, 0.04 ± 0.02 ($n = 3$); and for 1 mM ac-KIFMK-NH₂ with LqTx, 0.03 ± 0.02 ($n = 6$). (C) The fractional current (I_{12}/I_1) remaining after 10 conditioning pulses measured for channels blocked by 1 mM ac-KIFMK-NH₂ in the absence or presence of 100 nM LqTx applied to the extracellular side. The conditioning pulses were to 200 mV and the final interval at -80 mV between pulse 11 and 12 was lengthened to 91 s. The mean fractional recovery from use-dependent block by 1 mM ac-KIFMK-NH₂ in the absence of LqTx was 0.26 ± 0.05 ($n = 8$) and in the presence of 100 nM LqTx was 0.56 ± 0.04 ($n = 3$).

slowly reversible complex that forms after repetitive depolarizations to positive membrane potentials and is much more stable than fast inactivation.

Structural Features Affecting Use-dependent Peptide Block

Use-dependent block was measured using the pulse protocol illustrated in Fig. 4 for sodium channels not modified by LqTx (Fig. 5). Although both fast block and slow, use-dependent block occurred during the conditional pulse protocol, sodium channels recovered from fast block with a time constant of 0.9 ± 0.3 ms at -80 mV (see Fig. 2 B), and so they were not expected to affect our measurements of use-dependent block.

Ac-KIFMK-NH₂ (1 mM) produced use-dependent

block with half-maximal effect at $+125$ mV (Fig. 5 A). Varying the structure of pentapeptides containing both the IFM motif and two positive charges had profound effects on their potency for use-dependent block. The pentapeptide ac-RIFMR-NH₂ (Fig. 5 A, \square) exhibited use-dependent block using the conditional pulse protocol and was significantly more potent than ac-KIFMK-NH₂ (Fig. 5 A, \bullet). In contrast, the pentapeptide ac-KAFAK-NH₂ (Fig. 5 A, \blacktriangledown), in which the I and M of the IFM motif were replaced by alanines, was less effective. Previous results showed that ac-KIQMK-NH₂ was also ineffective in use-dependent block (Eaholtz et al., 1994). Thus, all three amino acid residues of the IFM motif are required for effective use-dependent block. However, DIFMK-NH₂ (Fig. 5 A, \diamond) and KIFMT-NH₂

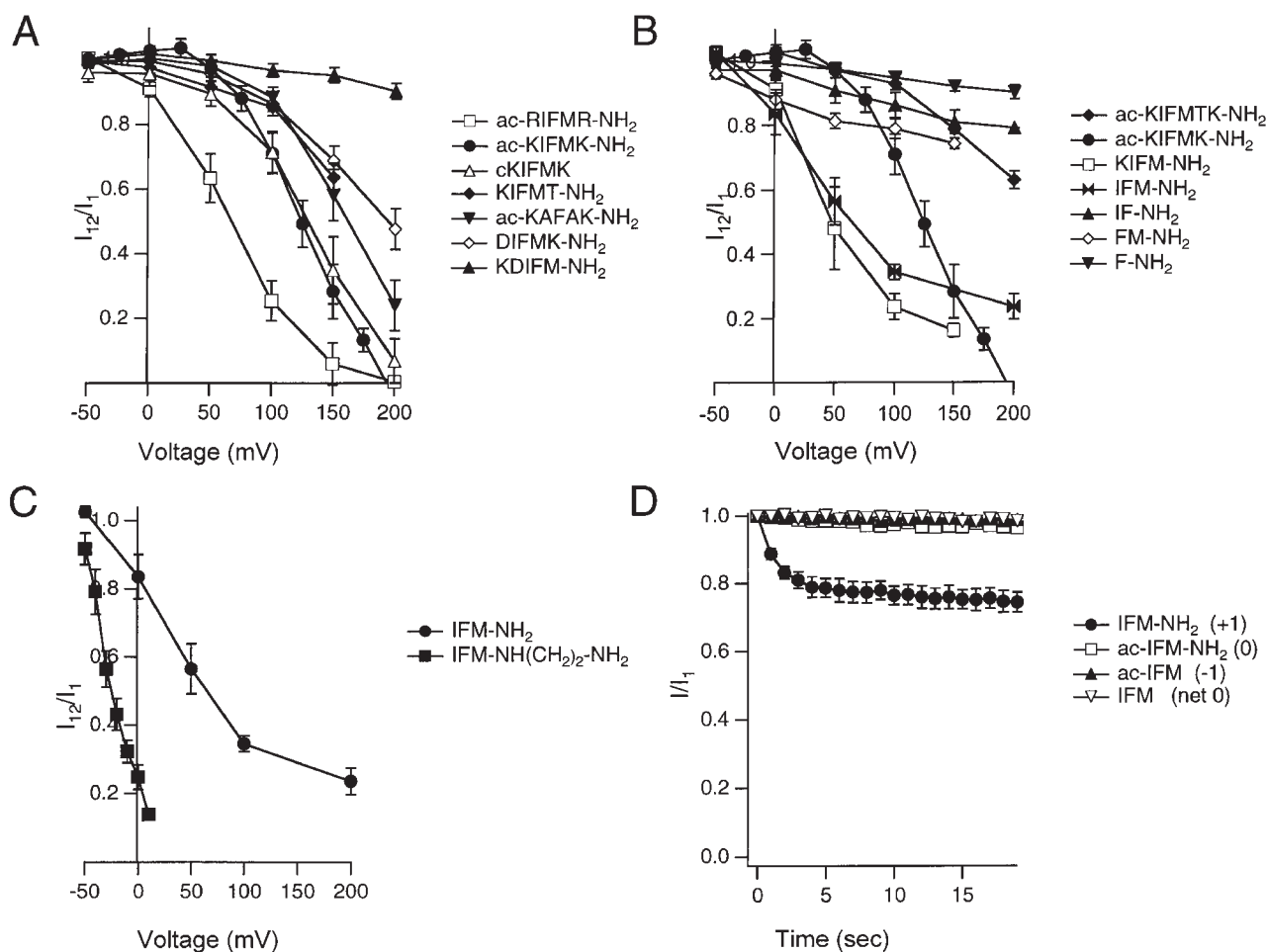


FIGURE 5. Effects of IFM-containing peptides on use-dependent block of sodium channels. (A–C) Fractional block (I_{12}/I_1) induced by intracellular solutions with 1 mM of an IFM peptide using the conditioning pulse protocol illustrated in Fig. 3 was plotted versus the voltage of the conditioning pulses. (D) Normalized sodium currents elicited by 10-ms test pulses to 0 mV from a holding potential of -80 mV at 1 Hz in the presence of 1 mM IFM peptides.

(Fig. 5 A, \blacklozenge), which contained either the natural asp preceding or the natural thr after the IFM motif, were much less effective than ac-KIFMK-NH₂. KDIFM-NH₂ was even less potent (Fig. 5 A, \blacktriangle), and ac-DIFMT-NH₂ had no effect at all (not shown). Thus, even though these asp and thr residues are present in the inactivation gate itself, their presence in these pentapeptides reduces use-dependent block. Cyclic KIFMK (Fig. 5 A, \triangle), which produced negligible fast block, was nearly as potent in use-dependent block as ac-KIFMK-NH₂, producing almost 100% block at 200 mV (Fig. 5 A). Evidently, its rigid structure is not an impediment to slow block during repetitive depolarizations, but prevents fast block on the millisecond time scale.

We examined larger and smaller peptides containing the IFM motif or parts of it to determine the minimum requirements for potent use-dependent block. Ac-KIFMTK-NH₂ (Fig. 5 B, \blacklozenge), which produced significant fast block, was a poor use-dependent blocker (Fig. 5 B), perhaps because it is too large to bind deeply within

the pore. The tetrapeptide KIFM-NH₂ (Fig. 5 B, \square) exhibited substantial use-dependent block, exceeding that of ac-KIFMK-NH₂ at 50 and 100 mV. The positively charged tripeptide IFM-NH₂ (Fig. 5 B, $\blacktriangleright\blacktriangleleft$) was also an effective use-dependent blocker, almost as potent as KIFM-NH₂. In contrast, the positively charged dipeptides IF-NH₂ (Fig. 5 B, \blacktriangle) and FM-NH₂ (\diamond) and the positively charged phe derivative F-NH₂ (\blacktriangledown) were not effective in use-dependent block. Since these smaller compounds are both hydrophobic and positively charged, it is evident that more than these minimal chemical properties are necessary to allow use-dependent block under the conditions studied here.

The tripeptides ac-IFM, IFM, ac-IFM-NH₂, and IFM-NH₂ have net charges of -1 , 0 (zwitterionic), 0 , and $+1$, respectively, and therefore provide a clear test of the importance of charge in use-dependent block. The positively charged IFM-NH₂ (Fig. 5 C, \bullet) was effective in use-dependent block. Depolarization to 0 mV at 1 Hz caused use-dependent block by IFM-NH₂ (Fig. 5 D, \bullet),

but did not induce significant block by ac-IFM (\blacktriangle), ac-IFM-NH₂ (\square), or IFM (∇). These results provide the most direct evidence for the requirement of positive charge for effective use-dependent block. To determine whether increased charge would increase the potency of an IFM tripeptide, we tested IFM-NH(CH₂)₂NH₂ (Fig. 5 C, \blacksquare) containing a positive charge on both sides of the IFM motif. This compound exhibited use-dependent block over a voltage range that was more negative than IFM-NH₂ or the larger peptides containing two positive charges. Nearly 80% of the channels were blocked by IFM-NH(CH₂)₂NH₂ (Fig. 5 C, \blacksquare) with con-

ditioning pulses to 0 mV. These results confirm that net positive charge is a crucial factor in determining blocking potency of IFM peptides, and show that the combination of the IFM motif and two positive charges is both necessary and sufficient for highly effective use-dependent block.

Effects of Changes in I, F or M Residues in the IFM Motif on Use-dependent Block of Wild-Type Sodium Channels

What structural features of the IFM motif contribute to the use-dependent blocking potency of peptides? It was

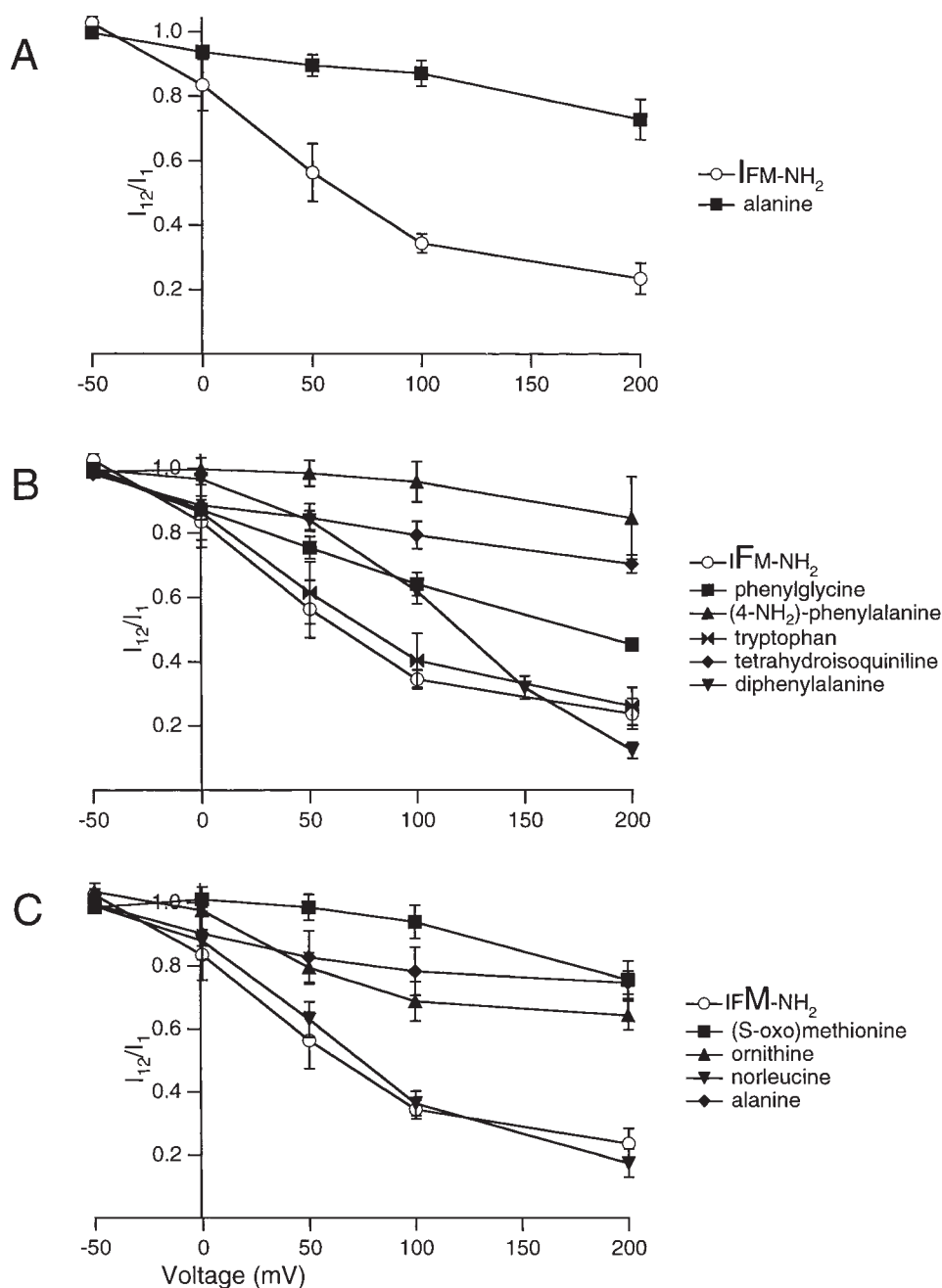


FIGURE 6. Effects of amino acid substitutions for I, F, or M on use-dependent block of sodium current. Mean fractional block (I_{12}/I_1) induced by 1 mM IFM peptide in the intracellular solution using the conditioning pulse protocol of Fig. 3 was plotted versus the voltage of the conditioning pulse. The mean fractional block values at 100 mV for each peptide shown are presented in Table II. (A) Substitutions for ile. (B) Substitutions for phe. (C) Substitutions for met.

shown previously that the peptides ac-KIQMK-NH₂ and ac-KAFK-NH₂ did not produce fast block of sodium channels (Eaholtz et al., 1994). Using the conditional pulse protocol, ac-KAFK-NH₂ produced significant use-dependent block of wild-type sodium channels (>60% at 200 mV; Fig. 5 A), but much less than ac-KIFMK-NH₂, while ac-KIQMK-NH₂ did not produce significant block (data not shown). To determine what other structural changes to the IFM motif affect use-dependent block, peptides were synthesized with substitutions of various natural and synthetic amino acids in IFM-NH₂, the minimal blocking peptide (Fig. 6, Table II).

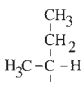
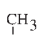
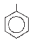


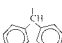
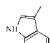
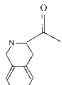
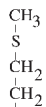
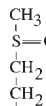
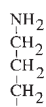
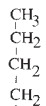
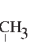
Substitution of ala for ile to yield the peptide AFM-NH₂ (Fig. 6 A, ■) substantially reduced use-dependent block at conditional pulse potentials from +50 to +200 mV compared with IFM-NH₂ (Fig. 6 A, ○). 87% of the current remained at 100 mV, compared with 34% for IFM-NH₂ (Table II). These results indicate that the larger, more hydrophobic ile residue gives more potent block.

Substitutions for met in the IFM-NH₂ peptide were made and analyzed similarly (Fig. 6 C; Table II). Substitution of norleucine (Fig. 6 C, ▼) produced ~64% block at 100 mV, leaving 36% of the current unblocked at steady state, similar to IFM-NH₂. In contrast, the less hydrophobic substitutions of ala (Fig. 6 C, ◆), ornithine (Fig. 6 C, ▲), and (S-oxo)-methionine (Fig. 6 C, ■) produced less block, leaving 78 ± 7%, 68 ± 6%, and 94 ± 5%, respectively, of the current unblocked at steady state at 100 mV (Table II). These results indicate that the interaction of met with the IFM binding site is also hydrophobic in nature.

The phenyl group within the IFM motif was necessary for the binding of the peptide to the channel and for rapid block during single pulses (Eaholtz et al., 1994). Substitution of trp (Fig. 6 B, ►◄) for phe yielded similar blocking potency as IFM-NH₂, with 40% unblocked at 100 mV. In contrast, substitution of the smaller but more hydrophilic 4-NH₂-phe (Fig. 6 B, ▲) caused nearly complete loss of blocking potency, suggesting the importance of hydrophobic interactions at this position of the tripeptide as well.

Other structural alterations revealed requirements for the size and conformation of the hydrophobic residues substituted for phe in IFM-NH₂. There was a size limitation on this hydrophobic interaction because substitution of the larger, more hydrophobic residue diphenylalanine (Fig. 6 B, ▼; Table II) resulted in a peptide that was significantly less potent than IFM-NH₂ at 100 mV. Substitution of phenylglycine (Fig. 6 B, ■; Table II), which places the phenyl ring nearer to the peptide backbone and in a constrained position, also produced substantially less block than IFM-NH₂. Tetrahydroisoquinoline (Fig. 6 B, ◆; Table II), in which the phenyl ring is even more restricted to a specific conformation, produced even less use-dependent block. These results con-

TABLE II
Structural Requirements for Use-dependent Block

Position	Substituent	Side chain	I ₁₂ /I ₁	n
I	Isoleucine		100 mV 0.34 ± 0.03	3
	Alanine		0.87 ± 0.04	4
F	Phenylglycine		0.64 ± 0.03	6
	Phenylalanine		0.34 ± 0.03	3
	(4-NH ₂)-Phenylalanine		0.95 ± 0.06	3
	Diphenylalanine		0.62 ± 0.04	3
	Tryptophan		0.40 ± 0.08	3
M	L-Tetrahydroisoquinoline*		0.79 ± 0.04	4
	Methionine		0.34 ± 0.03	3
	(S-oxo)-Methionine		0.94 ± 0.05	4
	Ornithine		0.68 ± 0.06	3
	Norleucine		0.36 ± 0.04	3
	Alanine		0.78 ± 0.07	3

*Structure represents the entire amino acid residue rather than just the side chain.

firm that the phenyl ring is an important determinant in the binding interaction between the IFM tripeptides and the sodium channel, and show that there is a substantial hydrophobic component to this interaction and a significant space and conformational restriction for binding of the phenyl ring of phe to its receptor site.

DISCUSSION

Two Forms of Peptide Block

Our experiments further characterize the block of sodium channels by IFM-containing peptides. These peptides block sodium channels by at least two distinguish-

able mechanisms that are referred to here as fast block and use-dependent block. Both types of block occur when the channel is open and require that peptides have a net positive charge. Fast block resembles the intrinsic inactivation of the sodium channel in its rapid kinetics of onset and reversal. Moreover, in previous work (Eaholtz et al., 1994), it was shown that binding of ac-KIFMK-NH₂ prevents the channel from entering into the inactivated state during depolarizing pulses and results in tail currents through the open channel when the membrane is repolarized. This suggests that IFM peptides compete with the intrinsic inactivation gate during fast inactivation and prevent it from securely inactivating the channel. Like inactivation, the rate of recovery from ac-KIFMK-NH₂ block is accelerated at more negative membrane potentials. However, the ac-KIFMK-NH₂-blocked state is less stable than the inactivated state since recovery is faster at the same membrane potential. This lack of stability may be a characteristic of a freely diffusible peptide, in contrast to the native channel where IFM, by virtue of its attachment to the rest of the protein, may be held in place more stably.

Many of the peptides produce slow use-dependent block during conditioning pulses to very positive membrane potential. This slowly reversible block is not observed during 10-ms pulses in channels with functional inactivation in the absence of peptide. Recovery from use-dependent block is much slower than recovery from the fast peptide block or from inactivation in the absence of peptide. However, the α -scorpion toxin LqTx, which slows fast inactivation, increased the rate of recovery from use-dependent block. This result suggests that use-dependent block is a stable form of block of inactivated sodium channels since its reversal is accelerated by a toxin that opposes fast inactivation.

The two different blocked complexes are distinguished by different values of δ , consistent with penetration of the charged moieties of ac-KIFMK-NH₂ to different depths in the pore. Measurements of the voltage dependence of fast block by KIFMK indicated a δ value of 0.3 (Eaholtz et al., 1998). In contrast, use-dependent block by ac-KIFMK-NH₂ has a δ value of 0.5. These results show that the charges on the peptides pass through a larger fraction of the electric field during slow, use-dependent block compared with fast block and therefore suggest that use-dependent block involves binding of the IFM peptide deeper in the pore.

Structural Requirements for Fast Block

The most prominent structural features of the peptides required for producing the fast block that resembles intrinsic channel inactivation are small size, the IFM motif, two positive charges, and conformational flexibility. When peptides contain six or fewer amino acid residues, the IFM motif, two positive charges, and a flexible

backbone, fast block of sodium channels is observed. Larger peptides are not effective fast blockers (Eaholtz et al., 1994), presumably because they cannot reach the inactivation gate receptor site rapidly enough. Flexibility of the linear peptides presumably enables them to adopt conformations suitable for block, whereas the fixed conformation of cyclic KIFMK is ineffective as a fast blocker because it does not allow binding to the inactivation gate receptor site in the pore of the sodium channel. These strict requirements for diffusible peptides of small size and specific conformation may reflect a narrow access pathway to the inactivation gate receptor when the intrinsic inactivation gate is in place. If the intrinsic inactivation gate could be removed from the channel, larger exogenously added peptides might be effective fast blockers.

Fast block requires the intact IFM motif. Substitution of ala for any of these three residues prevents fast block, as does substitution of gln for phe. Thus, the structure and hydrophobicity of the IFM motif provides the specificity and affinity for fast channel block by inactivation gate mimetics. However, the IFM motif is not sufficient. Fast block also requires two positive charges. This is a surprising finding because there are no positive charges near the IFM motif in the inactivation gate. The two positive charges can be placed in any position surrounding the IFM motif: at the ϵ -NH₂ position in lys, in the guanidinium of arg, at the α -NH₂ position of lys or ile, or in a COOH-terminal ethylenediamine moiety. Moreover, the two positive charges can be positioned on each side of the IFM motif or both on one side. The lack of positional specificity of the positive charges argues that they do not interact in a specific way with the inactivation gate receptor. Instead, we hypothesize that the two positive charges serve to concentrate the IFM peptides near the surface of the membrane at the intracellular mouth of the pore and thereby position the peptides for rapid access to the pore when the sodium channel opens. Murrell-Lagnado and Aldrich (1993) found similar effects with ShB peptides where substitutions that increased the net positive charge increased the on-rate constant of block and substitutions that preserved the net charge had little effect on the on- or off-rate constants of peptide block of noninactivating ShB4-64 potassium channels.

Structural Requirements for Use-dependent Block

Peptides that produce use-dependent block share some structural features with those that produce fast block, but a wider range of structures is effective. As for fast block, a positive charge is required, the size of the peptide is limited, and more hydrophobic peptides are more effective. In contrast to fast block, a single positive charge is sufficient and both restricted conformation and substitutions in the IFM motif are tolerated.

The requirement for positive charge is illustrated best by the effects of five different derivatives of the tripeptide IFM. Acetyl-IFM (charge of -1), acetyl-IFM-NH₂ (neutral), and IFM (zwitterionic) cause neither fast nor use-dependent block. In contrast, IFM-NH₂ (charge of $+1$ on the NH₂-terminal side) is an effective use-dependent blocker, but does not produce much fast block, while IFM-NH(CH₂)₂NH₂ (charge of $+2$ with charge on each side of IFM) is an effective fast blocker and the most potent use-dependent blocker. For use-dependent block, the positive charge may serve both to concentrate the peptide and to interact with its receptor site.

There is a less strict requirement for a specific amino acid sequence or conformation for IFM-containing pentapeptides to produce use-dependent block. At the most positive voltages tested, ac-KAFAK-NH₂ is an effective blocker (Fig. 5 A), but ac-DIFMT-NH₂ and ac-KIQMK-NH₂ are not (data not shown). As for fast block, ac-RIFMR-NH₂ is more potent than ac-KIFMK-NH₂. On the other hand, cyclic KIFMK produces almost as much use-dependent block as the flexible linear form ac-KIFMK-NH₂, in contrast to its ineffectiveness as a fast blocker.

Because the IFM-NH₂ is the simplest effective use-dependent blocker, we explored the effects of substitutions in this tripeptide in more detail. Substitution of smaller, less hydrophobic amino acid residues for ile or met substantially reduced potency for use-dependent block. Substitutions for phe indicated that the size, hydrophobicity, and conformation of this residue are all important. Decrease in hydrophobicity by substitution of 4-NH₂-phe greatly reduced potency for use-dependent block. Increase in size by substitution of trp gave a somewhat more potent blocker while substitution of the larger diphenylalanine moiety substantially reduced potency except at very high positive voltages. Evidently, the limiting size is between trp and diphenylalanine. Restriction of the conformational flexibility of the phenyl ring by substitution of phenylglycine or tetrahydroisoquinoline also substantially reduce the potency for block.

Relationship to Local Anesthetics

Use-dependent block by IFM-containing peptides resembles local anesthetic block of sodium channels (Strichartz, 1973; Hille, 1977; Cahalan, 1978; Yeh, 1978; Wang et al., 1987; Butterworth and Strichartz, 1990; Gringrich et al., 1993; Wang and Wang, 1994) and quaternary ammonium block of potassium channels (Armstrong, 1971; Holmgren et al., 1997). These compounds are thought to enter the intracellular mouth of the pore and bind stably to the inactivated state of sodium channels. When inactivation is modi-

fied with LqTx or with pronase (Cahalan, 1978), the drug-bound inactivated state is destabilized for some drugs and the rate of recovery from the use-dependent block is increased. Cahalan (1978) speculated that blocking compounds were being "trapped" by the functioning inactivation gate and, when the closure of the inactivation gate was prevented by toxin or proteolytic cleavage, the blocking molecule was no longer prevented from leaving the channel. However, disabling the inactivation gate with chloramine-T (Wang et al., 1987) or limited proteolysis (Yeh and TenEick, 1987) does not disrupt the actions of local anesthetics to produce use-dependent block, suggesting that substantial disruption of inactivation is required to destabilize the drug-bound, inactivated state.

Zamponi and French (1994) suggest that the minimal structural requirements for open-channel block by the local anesthetic lidocaine are (a) a charged amino group, (b) an aromatic ring, and (c) a somewhat flexible aryl-amine link. Wang (1990) also suggests, from block by stereoisomers, that the local anesthetic receptor has two separate subsites, one that binds the aromatic ring and one that binds the aminoalkyl group. The size of the hydrophobic pocket for the aromatic group is thought to be very large, 18–20 carbons (Wang et al., 1991). The idea of separate subsites for the aromatic and amino moieties is in agreement with the data of Zamponi and French (1993), who show that coapplication of phenol and diethylamide (the chemical constituents of lidocaine) does not alter block by diethylamide. The local anesthetic receptor site has been localized to transmembrane segment IVS6 of the sodium channel α subunit (Ragsdale et al., 1994). Phe1764 and tyr1771 are the two critical amino acid residues, and it was suggested that they form subsites for binding of the amino and aromatic moieties of the local anesthetics (Ragsdale et al., 1994). Mutations of these two amino acid residues do not have major effects on fast inactivation of sodium channels or on fast block by IFM peptides, so it is unlikely that these two residues form the inactivation gate receptor site (McPhee et al., 1995). Therefore, the receptor site for the local anesthetics and the receptor site that binds the IFM motif of the inactivation gate during fast inactivation must be different. Based on these results, we hypothesize that the site at which the IFM peptides bind during fast block of sodium channels is the inactivation gate receptor, consistent with their ability to prevent closure of the inactivation gate (Eaholtz et al., 1994). In contrast, during use-dependent block, these peptides may bind deeper in the pore either at the inactivation receptor site driven into a different conformation by the strong depolarizations or at a different receptor site that may overlap the local anesthetic receptor site. Two sequential sites of interaction have also been proposed for block of sodium

channels by tetraethylammonium derivatives (Gringrich et al., 1993). Stepwise binding of drugs to two sites in the pore may be a common property of differ-

ent ion channels, and may also be a property of the binding of IFM peptides to sodium channels.

The authors thank Mr. Carl Baker for purifying the LqTx used in these experiments. We also thank Drs. William N. Zagotta and Todd Scheuer for helpful discussions and comments on this manuscript. G. Eaholtz and W.A. Catterall thank Parke-Davis for their interest and generous support of this project.

This research was supported by National Institutes of Health research grant NS-15751 to W.A. Catterall and by a research grant and a predoctoral fellowship from Parke-Davis Research Division of Warner-Lambert Corp.

Original version received 9 June 1998 and accepted version received 23 November 1998.

REFERENCES

- Armstrong, C.M. 1971. Interaction of tetraethylammonium derivatives with the potassium channels of giant axons. *J. Gen. Physiol.* 58:413–437.
- Auld, V.J., A.L. Goldin, D.S. Krafte, W.A. Catterall, H.A. Lester, N. Davidson, and R.J. Dunn. 1990. A neutral amino acid change in segment IIS4 dramatically alters the gating properties of the voltage-dependent sodium channel. *Proc. Natl. Acad. Sci. USA.* 87: 323–327.
- Auld, V.J., A.L. Goldin, D.S. Krafte, J. Marshall, J.M. Dunn, W.A. Catterall, H.A. Lester, N. Davidson, and R.J. Dunn. 1988. A rat brain Na⁺ channel alpha subunit with novel gating properties. *Neuron.* 1:449–461.
- Bezanilla, F.M., and C.M. Armstrong. 1977. Inactivation of the sodium channel. I. Sodium current experiments. *J. Gen. Physiol.* 70: 549–566.
- Buttersworth, J.F., and G.R. Strichartz. 1990. Molecular mechanisms of local anesthesia: a review. *Anesthesiology.* 72:711–734.
- Cahalan, M.D. 1978. Local anesthetic block of sodium channels in normal and pronase-treated squid giant axons. *Biophys. J.* 21: 285–311.
- Catterall, W.A. 1976. Purification of a toxin from scorpion venom which activates the action potential sodium ionophore. *J. Biol. Chem.* 251:5528–5536.
- Catterall, W.A. 1992. Cellular and molecular biology of voltage-gate sodium channels. *Physiol. Rev.* 72:S15–S48.
- Eaholtz, G., T. Scheuer, and W.A. Catterall. 1994. Restoration of inactivation and block of open sodium channels by an inactivation gate peptide. *Neuron.* 12:1041–1048.
- Eaholtz, G., W.N. Zagotta, and W.A. Catterall. 1998. Kinetic analysis of block of open sodium channels by a peptide containing the isoleucine, phenylalanine, methionine (IFM) motif from the inactivation gate. *J. Gen. Physiol.* 111:75–82.
- Gringrich, K.J., D. Beardsley, and D.T. Yue. 1993. Ultra-deep blockade of Na⁺ channels by a quaternary ammonium ion: catalysis by a transition-intermediate state? *J. Physiol. (Camb.).* 471:319–341.
- Hamill, O.P., A. Marty, E. Neher, B. Sakmann, and F.J. Sigworth. 1981. Improved patch-clamp techniques for high-resolution current recording from cells and cell-free membrane patches. *Pflügers Arch.* 391:85–100.
- Hille, B. 1977. Local anesthetics: hydrophilic and hydrophobic pathways for the drug-receptor interaction. *J. Gen. Physiol.* 69: 497–515.
- Holmgren, M., P. Smith, and G. Yellen. 1997. Trapping of organic blockers by closing of voltage-dependent K⁺ channels: evidence for a trap door mechanism of activation gating. *J. Gen. Physiol.* 109:527–535.
- Kellenberger, S., T. Scheuer, and W.A. Catterall. 1996. Movement of the Na⁺ channel inactivation gate during inactivation. *J. Biol. Chem.* 271:30971–30979.
- McPhee, J.C., D.S. Ragsdale, T. Scheuer, and W.A. Catterall. 1995. A critical role for transmembrane segment IVS6 of the sodium channel α subunit in fast inactivation. *J. Biol. Chem.* 270:12025–12034.
- Miller, C. 1982. Bis-quaternary ammonium blockers as structural probes of the sarcoplasmic reticulum K⁺ channel. *J. Gen. Physiol.* 79:869–891.
- Mozhayeva, G.N., M. Naumov, N.M. Solatov, and E.V. Grishin. 1979. Effects of toxins from scorpions *Buthes eupeas* on the sodium channels of the membranes of nodes of Ranvier. *Biofizika.* 24:235–241.
- Murrell-Lagnado, R.D., and R.W. Aldrich. 1993. Interactions of amino terminal domains of *Shaker* K channels with a pore blocking site studied with synthetic peptides. *J. Gen. Physiol.* 102:949–975.
- Noda, M., T. Ikeda, T. Kayano, H. Suzuki, H. Takeshima, M. Kurasaki, H. Takahashi, and S. Numa. 1986. Existence of distinct sodium channel messenger RNAs in rat brain. *Nature.* 320:188–192.
- Patlak, J.B. 1991. Molecular kinetics of voltage-dependent Na⁺ channels. *Physiol. Rev.* 71:1047–1080.
- Patton, D.E., J.W. West, W.A. Catterall, and A.L. Goldin. 1992. Amino acid residues required for fast sodium channel inactivation. Charge neutralizations and deletions in the III–IV linker. *Proc. Natl. Acad. Sci. USA.* 89:10905–10909.
- Patton, D.E., J.W. West, W.A. Catterall, and A.L. Goldin. 1993. A peptide segment critical for sodium channel inactivation functions as an inactivation gate in a potassium channel. *Neuron.* 11: 967–974.
- Pusch, M., and E. Neher. 1988. Rates of diffusional exchange between small cells and a measuring patch pipette. *Pflügers Arch.* 411:204–211.
- Ragsdale, D.S., J.C. McPhee, T. Scheuer, and W.A. Catterall. 1994. Molecular determinants of state-dependent block of sodium channels by local anesthetics. *Science.* 265:1724–1728.
- Strichartz, G.R. 1973. The inhibition of sodium currents in myelinated nerve by quaternary derivatives of lidocaine. *J. Gen. Physiol.* 62:37–57.
- Stühmer, W., F. Conti, H. Suzuki, X. Wang, M. Noda, N. Yahagi, H. Kubo, and S. Numa. 1989. Structural parts involved in activation and inactivation of the sodium channel. *Nature.* 339:597–603.
- Vassilev, P.M., T. Scheuer, and W.A. Catterall. 1988. Identification of an intracellular peptide segment involved in sodium channel inactivation. *Science.* 241:1658–1661.
- Vassilev, P.M., T. Scheuer, and W.A. Catterall. 1989. Inhibition of inactivation of single sodium channels by a site-directed antibody. *Proc. Nat. Acad. Sci. USA.* 86:8147–8151.
- Wang, G.K., M.S. Brodwick, D.C. Eaton, and G.R. Strichartz. 1987.

- Inhibition of sodium current by local anesthetics in chloramine-T-treated squid axons. The role of channel activation. *J. Gen. Physiol.* 89:747–765.
- Wang, G.K. 1990. Binding affinity and stereoselectivity of local anesthetics in single batrachotoxin-activated Na⁺ channels. *J. Gen. Physiol.* 96:1105–1127.
- Wang, G.K., R. Simon, and S. Wang. 1991. Quaternary ammonium compounds as structural probes of single batrachotoxin-activated Na⁺ channels. *J. Gen. Physiol.* 98:1005–1024.
- Wang, G.K., and S. Wang. 1994. Binding of benzocaine in batrachotoxin-modified Na⁺ channels: state-dependent interactions. *J. Gen. Physiol.* 103:501–518.
- West, J.W., D.E. Patton, T. Scheuer, Y. Wang, A.L. Goldin, and W.A. Catterall. 1992. A cluster of hydrophobic amino acid residues required for fast Na⁺-channel inactivation. *Proc. Natl. Acad. Sci. USA.* 89:10910–10914.
- Woodhull, A.M. 1973. Ionic blockage of sodium channels in nerve. *J. Gen. Physiol.* 61:687–708.
- Yeh, J.Z. 1978. Sodium inactivation mechanism modulates QA-314 block of sodium channels in squid axons. *Biophys. J.* 24:569–574.
- Yeh, J.Z., and R.E. TenEich. 1987. Kinetic analysis of pancuronium interaction with sodium channels in squid axon membranes. *J. Gen. Physiol.* 69:293–323.
- Zamponi, G.W., and R.J. French. 1993. Dissecting lidocaine action: diethylamide and phenol mimic separate modes of lidocaine block of sodium channels from heart and skeletal muscle. *Biophys. J.* 65:2335–2347.
- Zamponi, G.W., and R.J. French. 1994. Amine blockers of the cytoplasmic mouth of sodium channels: a small structural change can abolish voltage dependence. *Biophys. J.* 67:1015–1027.

